JOURNAL OF AIRCRAFT
Vol. 44, No. 4, July–August 2007

Engineering Notes

ENGINEERING NOTES are short manuscripts describing new developments or important results of a preliminary nature. These Notes should not exceed 2500 words (where a figure or table counts as 200 words). Following informal review by the Editors, they may be published within a few months of the date of receipt. Style requirements are the same as for regular contributions (see inside back cover).

Modeling the Benchmark Active Controls Wing Through Linear and Computational Aeroelastic Analyses

N. V. Taylor,* A. L. Gaitonde,* D. P. Jones,* and C. B. Allen†
University of Bristol,
Bristol, BS8 1TH England, United Kingdom

DOI: 10.2514/1.22959

I. Introduction

FLUTTER has the potential to cause extremely rapid and catastrophic failure of aircraft structures. The prediction and analysis of this phenomena is therefore of critical importance, but also poses serious problems in the transonic region, in which nonlinear flows occur. For this reason, advanced computational aeroelastic (CAE) methods are under widespread development (e.g., [1–6]). These methods allow both the structure and aerodynamics to be modeled through nonlinear equations, increasing model fidelity, although at a far higher cost in terms of CPU time than traditional linear schemes. The CAE approach has been shown to be effective in the somewhat restricted set of currently available test cases with experimental data available for comparison. The AGARD445.6 wing, for example, has been simulated by a large number of workers, generating results with good accuracy (over the subsonic range at least; see [7,8] for recent overviews of these data). However, this wing is virtually the only test case used for validation of CAE codes with an experimental flutter boundary.

However, this is not the only wing with data relating to transonic flutter behavior in the literature available for comparison: the benchmark active controls (BACT) wing was tested in the mid 1990s, and data describing the flutter boundary were published in 1997 [9]. The wing was designed primarily for the investigation of active control for flutter suppression, and this meant that the main wing and dynamic system was designed to be as simple to model as possible [9], with the intention that linear analysis would provide an accurate representation of the behavior so that control laws based on classical analysis techniques could be implemented on the modeled system. A linearized model of the system was developed [10,11] and successfully used as the basis for a wide range of control law derivations (e.g., [12–15]).

A second motivation for the work was to generate a data set of results for validation of computational fluid dynamics (CFD) schemes on unsteady aerodynamic effects of actuators (specifically, a flap and spoilers [9,16]). These have been used for this purpose with Navier–Stokes codes [17,18] and comparison between linear and CFD schemes [19]; however, in all cases, it has been the effect on a rigid wing of actuator motion that was under consideration, not a simulation of the flutter boundary. The only simulation of the flutter boundary of the BACT wing currently available in the literature from a time-marching solution was made by a code that uses a transpiration velocity to represent surface motion [5]; however, the majority of CAE codes are based on mesh motion schemes, whereby the physical movement of the wing is realized within the computational domain. To the best of the authors' knowledge, no published results from such a scheme for this wing exist.

This may be explained in part by the success of the linear model applied to the wing; the wing was designed to be amenable to linear analysis techniques, and hence applying the more complex CAE techniques could be seen as somewhat redundant, because this should represent a relatively simple flow for the advanced coupled codes to solve. However, not only is the linearized method highly localized in nature, but significant differences in flutter boundary between simulation and experiment were found both with the previously mentioned transpiration method [5] and an unpublished study using an Euler-based moving mesh scheme [20] (although the former did, with some adjustments, produce some reasonable results, as will be discussed next). Furthermore, the AGARD445.6 wing is thin (only 4% thickness), which delays nonlinear effects to high subsonic Mach numbers, and is not representative of modern aircraft wing design. Although for different reasons, the same could be said of the BACT section, given the lack of alternative experimental data for validation and the importance of such validation, it is perhaps surprising that few have attempted simulation of the BACT wing.

Because the University of Bristol CAE coupled code USCRANSMB has demonstrated effective modeling capability for other widely known test cases [21–23], it was decided to use this code to investigate the BACT wing in an effort to determine the reasons for the anomalies mentioned earlier. This was done as part of a wider project to extend the code to allow aeroservoelastic analysis [24], of which the BACT wing is the principal extant test case with experimental results. In the process of this investigation, a number of interesting results emerged, discussed in detail next. Comparison is also made with the linearized model discussed in [10].

II. BACT Wing

Because of the focus on control surface dynamics and effects, the aerodynamic and structural behavior of the main wing were deliberately designed to be as simple as possible to analyze. The main aerodynamic structure is therefore extremely stiff, being primarily constructed from a solid block of aluminum ($E = 70.0 \times 10^9$ N/m^2, $\nu = 0.3$, and $\rho = 2700.0$ kg/m^3). The wing itself is symmetric, of a NACA0012 profile, with an aspect ratio of 2. The majority of the experimental results available, including the flutter boundary, were derived from tests conducted using the heavy gas R12 ($\gamma = 1.14$) as the working fluid.

The solid construction meant that when the root of the wing was fixed, it behaved in a nearly rigid manner. However, to allow aeroelastic analysis, the wing and a splitter plate were attached to the pitch and plunge apparatus (PAPA) mount. The very high stiffness of the main wing meant that when mounted on the PAPA, the dynamic behavior was greatly simplified and could be represented as a simple two-degree-of-freedom mass-spring system. The resulting wing and mount properties are given in Table 1.

Received 3 February 2006; accepted for publication 28 March 2007.

*Lecturer, Aerospace Department, Queens Building. Member AIAA.
†Reader, Aerospace Department, Queens Building. Member AIAA.

Table 1 BACT wing and PAPA mount properties

BACT wing and PAPA mount	English	SI
Span	32 in.	0.8128 m
Chord	16 in.	0.4064 m
Ref area	512 in.^{2}	0.3303 m^2
Plunge stiffness, K_ξ	2686 lb/ft	39,211 N/m
Plunge damping ratio	0.0014	0.0014
Pitch stiffness, K_α	3000 ft · lb/rad	4100 Nm/rad
Pitch damping ratio	0.001	0.001
Mass	6.08 slugs	88.70 kg
Pitch inertia	2.8 slug · ft^2	3.79 kg · m^2

III. Computational Model Description

A. Aerodynamic Model

USCRANSMB was developed at the University of Bristol by extending the BAESYSTEMS code RANSMB, a cell-centered finite volume solver of a Jameson type [25], to allow fully implicit unsteady calculations through the use of pseudotime stepping [26,27] on structured multiblock grids. Either Navier–Stokes or Euler equations may be solved. However, principally due to time constraints, only the Euler equations are solved in the current work. Time integration is through a modified Runge–Kutta scheme due to Melson et al. [28].

B. Structural Model

The structural solution for the work presented in this paper is based on linear modal analysis, making use of a prerun NASTRAN analysis of the BACT wing in a similar fashion to that used previously for effective analysis of the AGARD445.6 and MDO wings. The wing is modeled with plate elements. When simulating the rigidly mounted BACT wing, all root nodes are fully restrained. The PAPA mount is modeled by connecting all root nodes rigidly to one of a pair of nodes, the other being fully restrained. Springs of stiffnesses equal to the reported experimental values (see Table 1) then connect the two initially coincident nodes. The mass of the PAPA mount is included via a rigid connection to a mass placed such that the resulting inertia in heave and pitch are equal to the published values, and the center of gravity was located initially at a point that resulted in a pitch plunge coupling of the same value as the experiment (i.e., 0.028 in. rearwards of the elastic axis [5]). The frequencies of heave and pitch motion using this model are 3.34 and 5.24 Hz, comparing well with the experimentally derived values of 3.34 and 5.21 Hz.

C. Coupling Method

Communication of displacement and loads between the CFD and CSD modules is achieved via tight coupling [29] (i.e., synchronization of structural and aerodynamic solutions in real time). The transfer of loads and displacements from structural to aerodynamic solver (and vice versa) is problematic, because the two grids have differing node numbers and locations. Not only this, but the surfaces on which these nodes are defined are not generally the same. This difficulty is overcome in USCRANSMB via a two-stage interpolation process based on a hybrid constant volume tetrahedra [30] thin-plate spline [31,32] method. A thorough investigation of the interpolation from intermediate to aerodynamic grids on airfoil configurations has shown that the thin-plate spline is accurate and robust when the leading and trailing edges are contained in the intermediate grid [33]. Recent work has highlighted the importance of the transfer mechanism in aeroelastic solution process and demonstrated it to be a key factor in ensuring similarity of predictions between various codes [34,35].

Once the structural grid position is used to define the aerodynamic surface, the motion of this surface is communicated into the main volume grid through a hybrid spring-transfinite interpolation approach [36]. Grid speeds are then calculated to second-order accuracy.

IV. Aerodynamic Solution Grids

The BACT wing is rectangular, measuring 0.406 m in chord and 0.812 m in span. As previously mentioned, it has a constant NACA0012 airfoil section. The aerodynamic surface mesh was created using an algebraic scheme, and the CH multiblock volume grid was derived through the use of transfinite interpolation. The surface grid contained 161 points around the airfoil section and 29 spanwise sections, the tip being closed over the last two spanwise cells linearly (more realistic but complex meshes, with a rounded tip, were found to little change the flutter behavior). The volume grid extended 20 chord lengths to the outer boundaries in the x–z plane and four spans outwards from the wing tip (this being the distance to the tunnel wall; however, running with greater distance, or a symmetrical flow boundary condition at this boundary, was not found to make any difference to the results). The total number of cells was approximately 570,000. A mesh refinement exercise demonstrated that this grid was converged with respect to the steady flows.

V. Steady Results

A large part of the experimental results presented in [9] were derived from the model when locked rigidly at the root (i.e., with no motion in the PAPA mount). Initial comparison with experimental results for the wing demonstrated that the Euler code was behaving as expected, producing good results for low incidences (Figs. 1a, 1b, 2a, and 2b), although as can be seen, prediction of peak suction very near the tip was somewhat underestimated.

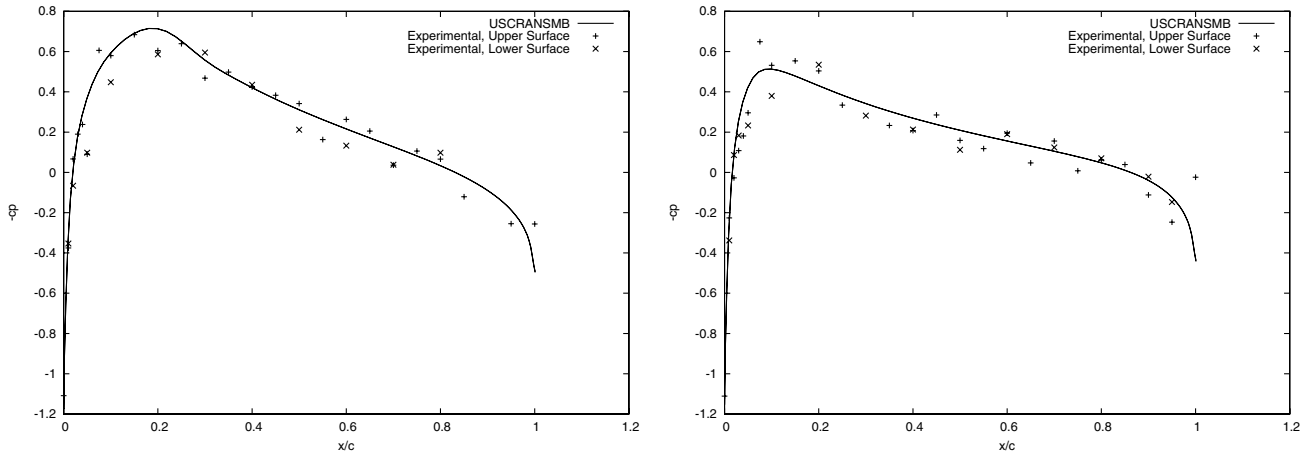

a) $\eta = 0.6$ b) $\eta = 0.95$

Fig. 1 Comparison with experimental data; $M = 0.77$ and $\alpha = 0.0$.

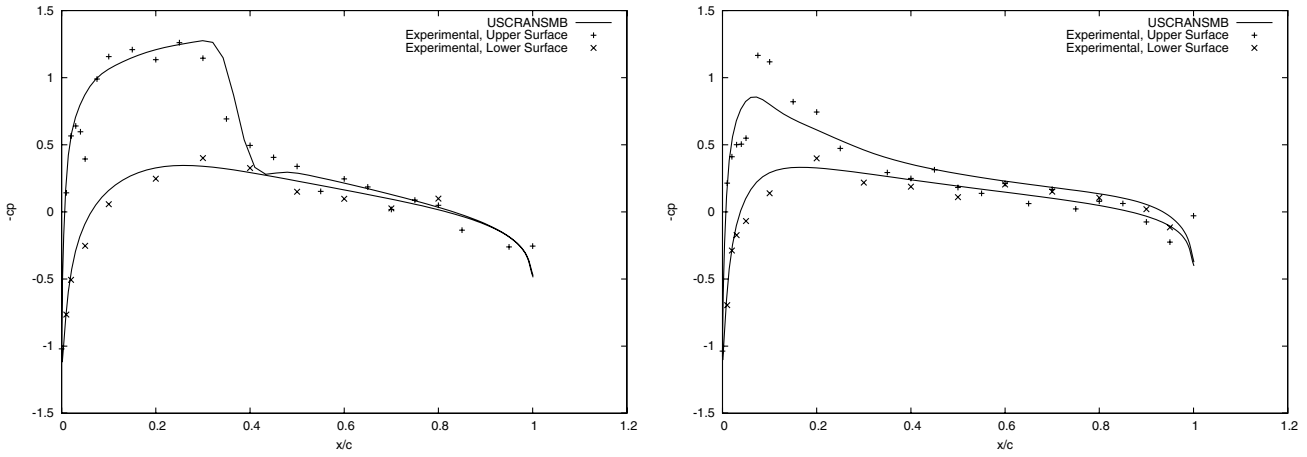

a) $\eta = 0.6$ b) $\eta = 0.95$

Fig. 2 Comparison of experimental and simulated flutter boundaries.

VI. Flutter Calculations

A. Coupled Flutter Boundary

The experimental flutter points were found with the BACT wing mounted on the PAPA mount and the flap locked in position, hence the wing was approximated in the structural model as a solid block of aluminum. Six modes were calculated using a NASTRAN analysis, the first two being the heave and pitch modes of the PAPA mount (3.34 and 5.24 Hz, as already mentioned), and four modes representing the wing itself were calculated at 57.4, 262.7, 329.8, and 351.5 Hz (these high values demonstrate the stiffness of the wing and would be expected to have minimal impact on the dynamic response).

The calculation of each flutter point initially was achieved at a nominal turntable angle of 2 deg to match that reported as typical of the experimental results [9]. All other conditions (including damping) were at the reported values. Motion was initiated by a modal excitation of the second (pitch) mode at a modal velocity of 0.1. The response of the modes and the heave and pitch of the wing tip could then be calculated over a number of time steps and, hence, the flutter speed determined.

The calculated flutter boundary is shown in Fig. 3. As may be seen, the initial calculation underpredicted the experimental flutter boundary by approximately 5% up to a Mach number of about 0.7, from whence a significant rise in flutter speed with Mach number is predicted, without any transonic dip. Although reasonable when compared with other coupled flow solvers (e.g., [20], in which a 100% overprediction at subsonic Mach numbers was noted, and [5], in which, for the reported experimental structural parameter conditions, a 10–15% overprediction of flutter speed was found), this still represents poor performance when compared with results for the code when applied to other test cases [21,23]. The effect of the time step and number of time steps simulated on the flutter boundary was investigated (Fig. 4), but found to be minor. Given this, an alternative explanation was sought, as discussed next. First, however, comparison is made to the linearized model, because this process provides some insight into the mechanisms causing the errors.

B. Linear Calculations

The linear equations presented in [10] may be used to estimate the flutter dynamic pressure of the BACT wing, given a set of structural and aerodynamic parameters. Because of the globally nonlinear nature of these parameters, the resulting model will only be valid locally, near to whatever conditions were used to derive the aerodynamic coefficients. Some of the coefficients reported in [10] were based on experimental data obtained at a Mach number and dynamic pressure of $M = 0.77$ and $q = 143$ psf; however, the unsteady coefficients needed were derived from an interaction of structures, aerodynamics, and controls (ISAC) program analysis at the same conditions, which is essentially a linear aerodynamic model. Aerodynamic coefficients at the same conditions were also derived from the USCRANSMB code for the BACT wing from forced motion calculations at the experimental flutter frequency (approximately 4 Hz) and substituted into the same linearized equations. This allowed some separation of the error caused by the coupling effects in the CAE solution from that due to the flow solution itself. The coefficients are shown in Table 2 with the data used in [11]. Numbers from this reference derived from experimental data are in bold, and other coefficients derive from the ISAC analysis.

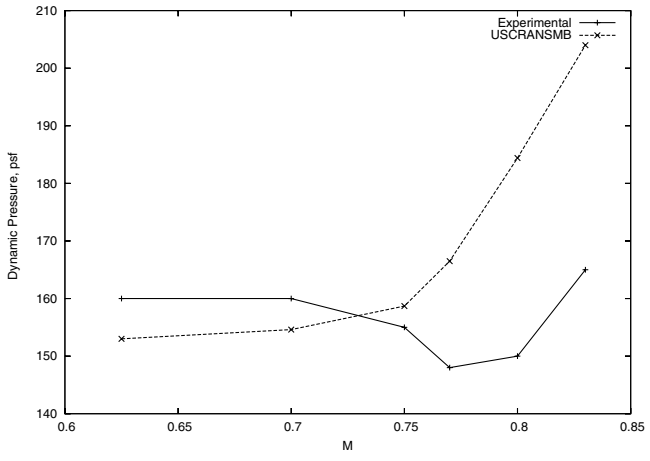

Fig. 3 Comparison of experimental and nonlinear flutter boundaries.

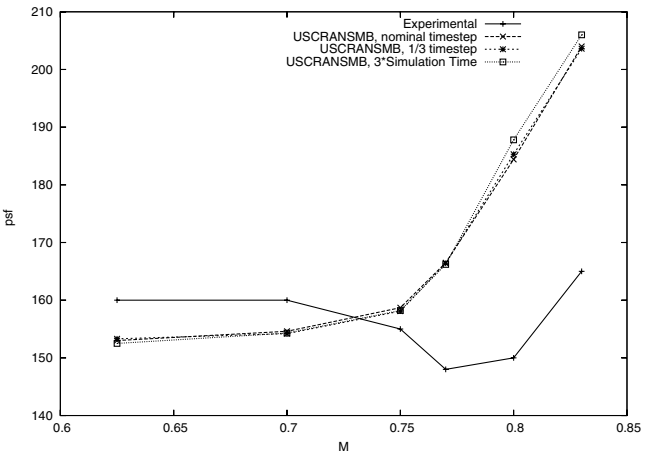

Fig. 4 Effect of the time step on the flutter boundary.

Table 2 BACT wing and aerodynamic properties

Property	Description	[10]	USCRANSMB
C_{L0}	Lift at zero angle of attack	0	0
C_{M0}	Pitching moment at zero angle of attack	0	0
$C_{L\alpha}$	Lift curve slope	**4.584**	5.097
$C_{M\alpha}$	Moment curve slope	**1.490**	0.1662
$C_{L\dot{\alpha}}$	Plunge damping due to the angle-of-attack rate	−3.1064	−7.23
C_{Lq}	Plunge damping due to the pitch rate	2.5625	0.689
$C_{M\dot{\alpha}}$	Pitch damping due to the angle-of-attack rate	−2.6505	−3.876
C_{Mq}	Pitch damping due to the angle-of-attack rate	−0.4035	−0.2979
l	Distance between the shear center and aerodynamic center, % chord	**−17.5**	−27.5

The flutter speed at $M = 0.77$ reported in [10] is 150.8 psf, compared with 148 psf from the experimental results. Using the data and equations provided by this reference, a model was created in MatLab that predicted a flutter speed of 150.9 psf; sufficiently similar that the discrepancy may be ascribed to a variation in the assumed speed of sound of the R12 gas, which was not reported for the experiment or numerical models and is assumed here to be 492 ft/s (130 m/s). When the coefficients derived from USCRANSMB were put into the model described in this paper, the flutter speed increased to 171.7 psf, an overprediction of some 30%. However, as may be seen, this is in reasonable agreement with the flutter speed predicted by the full simulation, using the same aerodynamic grid and boundary conditions as those used to derive the unsteady coefficients of 166.5 psf. It should be remembered that the aerodynamic data in Table 2 were derived from a dynamic pressure of only 143 psf, which would contribute to some of the discrepancy at the flutter point. (Note also that as would be expected, the flutter point provided by the linearized models are essentially invariant with Mach number, because no mechanism exists in the technique to allow for the variation of coefficients with velocity.)

C. Sensitivity to Physical Parameters

As noted earlier, an analysis of this test case using a CFD–CSD scheme based on a transpiration code (STARS) found an even larger difference between the simulation and experiment [5]. A possible cause of the discrepancy was suggested: small variations in the location of the elastic axis and center of gravity were found to have a significant effect on the flutter behavior of the wing (from p analysis, it was found that moving the center of gravity rearwards by only 0.25% of its nominal value reduced the flutter boundary by about 12.5%, and moving the center of gravity by a further 1% reduced the boundary by a total of 25%). As demonstrated in Fig. 5, a similar effect was found to exist for the coupled code.

However, when the center of gravity was moved in the USCRANSMB code, only small changes in flutter behavior were detected (Fig. 5). It therefore seems that the extreme sensitivity to center-of-gravity position reported for the STARS code and p method in [5] is lacking in the USCRANSMB model, with only a 2.0% change in flutter dynamic pressure at $M = 0.77$. Further, moving the center of gravity position on the linear model produced only a 2.1 and 2.6% variation in the flutter boundary position at $M = 0.77$ using the aerodynamic coefficients of [10] and those reported here, respectively.

Finally, Figs. 6 and 7 show the effect of damping, the size of the disturbance used to initiate the unsteady motion, and turntable incidence. As may be seen, the effect of damping at the levels reported is minimal, as is the size of the initial disturbance. The angle at which the turntable is set (θ_T), however, has a noticeable effect. As the incidence increases at low Mach numbers, the wing becomes less stable, whereas at higher (but still subsonic) Mach numbers, the dynamic pressure at which flutter occurs is increased. It is hypothesized that this is because at low Mach numbers, for which shock waves do not exist, increasing incidence increases the pressure

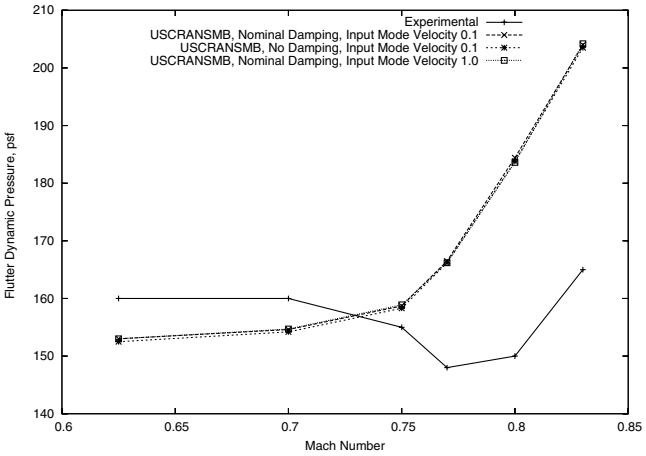

Fig. 6 Effect of damping and initiation velocity on flutter boundary, nominal 2^0 initial incidence.

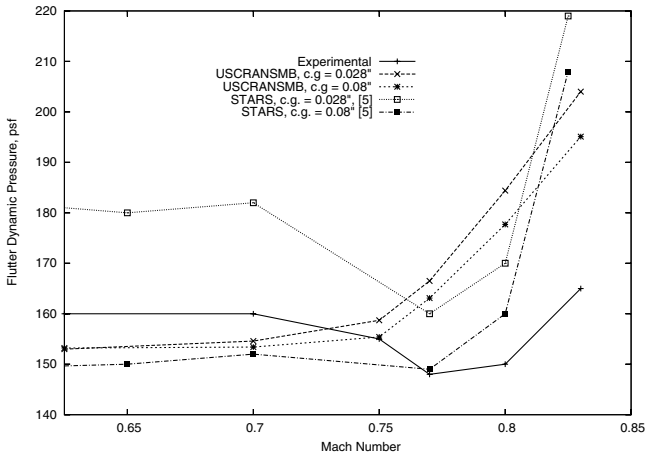

Fig. 5 Effect of the center of gravity position on flutter boundaries.

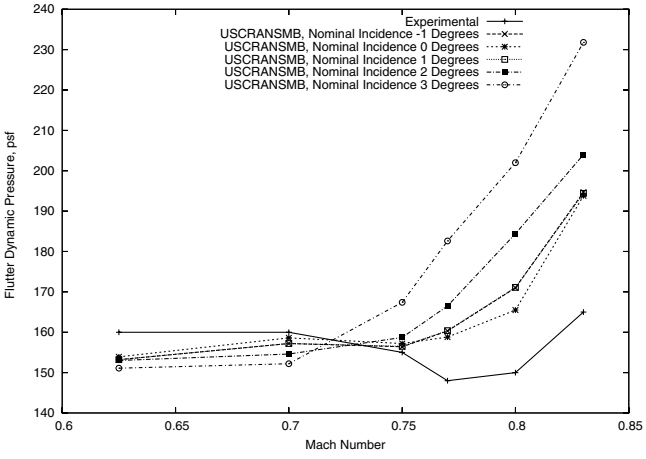

Fig. 7 Effect of nominal incidence on the flutter boundary.

peak at the leading edge, destabilizing the wing, whereas beyond the critical Mach number, increasing incidence strengthens the shock waves present in the analysis, and because the motion of these flow phenomena act as to damp the oscillation, the stronger shocks increase the flutter boundary (note that due to the symmetrical nature of the BACT airfoil section, it is the magnitude, not direction, of the turntable incidence that is important). Because Euler codes tend to overestimate shock strength, this explains the overprediction of the flutter boundary on this (and other) wings for such codes beyond the transonic dip. The effect is greater on the BACT wing than, for instance, the AGARD445.6 wing because of its unswept platform and moving root. This causes the majority of the span to be affected by any shock wave that forms, rather than just a small outboard region. For this reason the "artificial" damping produced by the overstrength shock waves would have a greater, and more immediate (in terms of Mach number range), effect on this wing.

Boundary conditions on the Euler code also provide a second source of error, both in shock behavior and critical Mach number prediction. The coupled calculations presented herein have not included the effects of the tunnel itself at the far-field boundary conditions, due to the difficulty in modeling slotted walls, and hence it is at least possible that some interference from the tunnel is altering the behavior of the BACT wing at the start of the transonic dip. Although no such problems are typically encountered when simulating the flutter boundary of the AGARD445.6 wing (tested in the same tunnel), that wing, although of similar plan area, is much thinner.

VII. Conclusions

A moving mesh coupled code USCRANSMB was applied to the BACT wing test case. Although the size and Mach range of the transonic dip are underpredicted and high subsonic flutter speeds are overpredicted, the errors are generally less than those present in the small reported number of similar simulation attempts. An examination of the reasons for the underprediction of the transonic dip has not supported a previous hypothesis, but has shown some evidence for an alternative: namely, that the principal problem is overprediction of shock wave strength. This work has shown the importance of experimental validation in gaining insight into the fundamental performance of coupled codes, because a simulation code that performs adequately on the usual test cases has, like other codes before, struggled on this apparently simpler test case. However, due to certain aspects of the design of the wing (particularly, its small aspect ratio and all-moving surface), the BACT wing has proved to be a demanding test. Work continues in improving the aerodynamic solution and understanding the mechanisms of transonic flutter.

References

[1] Alonso, J., and Jameson, A., "Fully-Implicit Time-Marching Aeroelastic Solutions," AIAA Paper 94-0056, 1994.

[2] Guruswamy, G., "Unsteady Aerodynamic and Aeroelastic Calculations for Wings Using Euler Equations," *AIAA Journal*, Vol. 28, No. 3, Mar. 1990, pp. 461–469.

[3] Meijer, J. J., Hounjet, M. H. L., Eussen, B. J. G., and Prananta, B. B., "NLR-TU Delft Experience in Unsteady Aerodynamics and Aeroelastic Simulation Applications," *Numerical Unsteady Aerodynamic and Aeroelastic Simulation*, AGARD Rept. R-822, Mar. 1998, pp. 11-1–11-21.

[4] Lee-Rausch, E. M., and Batina, J. T., "Wing Flutter Boundary Prediction Using Unsteady Euler Aerodynamic Method," *Journal of Aircraft*, Vol. 32, No. 2, Mar.–Apr. 1995, pp. 416–422.

[5] Stephens, C. H., Arena, A. S. Jr.,, and Gupta, K. K., "CFD-Based Aeroservoelastic Predictions with Comparisons to Benchmark Experimental Data," AIAA Paper 99-0766, 1999.

[6] Kandil, O. A., Massey, S. J., and Sheta, E. F., "Structural Dynamics-CFD Interaction for Computation of Vertical Tail Buffet," *The Aeronautical Journal*, Vol. 100, Aug.–Sept. 1996, pp. 297–303.

[7] Gordnier, R. E., and Melville, R. B., "Transonic Flutter Simulations Using an Implicit Aeroelastic Solver," *Journal of Aircraft*, Vol. 37, No. 5, 2000, pp. 872–879.

[8] Dowell, E., Edwards, J., and Strganac, T., "Nonlinear Aeroelasticity," *Journal of Aircraft*, Vol. 40, No. 5, Sept.–Oct. 2003, pp. 857–873.

[9] Scott, R. C., Hoadley, S. T., Wieseman, C. D., and Durham, M. H., "Benchmark Active Controls Technology Model Aerodynamic Data," *Journal of Guidance, Control, and Dynamics*, Vol. 23, No. 5, Sept.–Oct. 2000, pp. 914–921; also AIAA Paper 97-0829, 1997.

[10] Waszak, M. R., "Modeling the Benchmark Active Control Technology Wind-Tunnel Model for Active Control Design Applications," NASA TP-1998-206270, June 1998.

[11] Waszak, M. R., "Modeling the Benchmark Active Control Technology Wind-Tunnel Model for Application to Flutter Suppression," AIAA Paper 96-3437, 1996.

[12] Mukhopadhyay, V., "Transonic Flutter Suppression Control Law Design and Wind-Tunnel Test Results," *Journal of Guidance, Control, and Dynamics*, Vol. 23, No. 5, Sept.–Oct. 2000, pp. 930–937.

[13] Kelkar, A. G., and Joshi, S. M., "Passivity-Based Robust Control with Application to Benchmark Active Controls Technology Wing," *Journal of Guidance, Control, and Dynamics*, Vol. 23, No. 5, Sept.–Oct. 2000, pp. 938–947.

[14] Barker, J. M., and Balas, G. S., "Comparing Linear Parameter-Varying Gain-Scheduled Control Techniques for Active Flutter Suppression," *Journal of Guidance, Control, and Dynamics*, Vol. 23, No. 5, Sept.–Oct. 2000, pp. 948–955.

[15] Waszak, M. R., "Robust Multivariable Flutter Suppression for Benchmark Active Control Technology Wind-Tunnel Model," *Journal of Guidance, Control, and Dynamics*, Vol. 24, No. 1, Jan.–Feb. 2000, pp. 147–153.

[16] Bennett, R. M., Scott, R. C., and Wieseman, C. D., "Computational Test Cases for the Benchmark Active Controls Technology Model," *Journal of Guidance, Control, and Dynamics*, Vol. 23, No. 5, Sept.–Oct. 2000, pp. 922–929.

[17] Bartels, R. E., "An Elasticity-Based Mesh Scheme Applied to the Computation of Unsteady Three-Dimensional Spoiler and Aeroelastic Problems," AIAA Paper 99-3301-CP, 1999.

[18] Bartels, R. E., and Schuster, D. M., "Comparison of Two Navier–Stokes Methods with Benchmark Active Control Technology," *Journal of Guidance, Control, and Dynamics*, Vol. 23, No. 6, Nov.–Dec. 2000, pp. 1094–1099.

[19] Roughen, K. M., Baker, M. L., and Fogarty, T., "Computational Fluid Dynamics and Doublet-Lattice Calculation of Unsteady Control Surface Aerodynamics," *Journal of Guidance, Control, and Dynamics*, Vol. 24, No. 1, Jan.–Feb. 2000, pp. 160–166.

[20] O'Neill, C., "Euler3d Validation with the BACT Aeroelastic Test Case," *Computational Aeroservoelasticity (CASE) Lab* [online database], http://www.caselab.okstate.edu/ocharle/projects/validate-public.pdf [retrieved 27 October 2005].

[21] Taylor, N. V., Allen, C. B., Gaitonde, A. L., and Jones, D. P., "A Structure Coupled CFD Method for Time Marching Flutter Analysis," *The Aeronautical Journal*, Vol. 108, No. 1084, 2004, pp. 389–401.

[22] Taylor, N. V., Allen, C. B., Jones, D. P., Gaitonde, A. L., and Hill, G. F. J., "Investigation of Structural Modeling Methods for Aeroelastic Calculations," AIAA Paper 2004-5370, 2004.

[23] Taylor, N. V., Jones, D. P., Allen, C. B., Badcock, K. J., Woodgate, M. A., Rampurawala, A. M., Cooper, J. E., Vio, G. A., and Henshaw, M. J. de C., "A Comparison of Linear and Nonlinear Flutter Prediction Methods: A Summary of PUMA DARP Aeroelastic Results," Royal Aeronautical Society Paper 28, Sept. 2004.

[24] Taylor, N. V., Allen, C. B., Gaitonde, A. L., Jones, D. P., Fenwick, C. L., and Hill, G. F. J., "Moving Mesh CFD–CSD Aeroelastic Modeling of the BACT Wing with Autonomous Flap Control," 23rd Applied Aerodynamics Conference, AIAA Paper 2005-4840, 2005.

[25] Jameson, A., Schmidt, W., and Turkel, E., "Numerical Solutions of the Euler Equations by Finite Volume Methods Using Runge–Kutta Time Stepping Schemes," AIAA Paper 81-1259, 1981.

[26] Jameson, A., "Time Dependent Calculations Using Multigrid, with Applications to Unsteady Flows Past Airfoils and Wings," AIAA Paper 91-1596, 1991.

[27] Gaitonde, A., "A Dual-Time Method for the Solution of the Unsteady Euler Equations," *The Aeronautical Journal*, Vol. 98, No. 978, Oct. 1994, pp. 283–291.

[28] Melson, N. D., Sanetrik, M. D., and Atkins, H. L., "Time-Accurate Navier–Stokes Calculations with Multigrid Acceleration," NASA CP 3224, 1993.

[29] Vlachos, N., "Aero-Structural Coupling in Transonic Flow: Comparison of Strong and Weak Coupling Schemes," Defence Evaluation and Research Agency, Rept. ASF/3662U–AERO.RK5615, May 1999.

[30] Goura, G., "Time Marching Analysis of Flutter Using Computational Fluid Dynamics," Ph.D. Thesis, Dept. of Aerospace Engineering, Glasgow Univ., Glasgow, Scotland, U.K., 2001.

[31] Duchon, J., *Splines Minimising Rotation-Invariant Semi-Norms in Sobolev Spaces*, Constructive Theory of Functions of Several Variables, Springer, Berlin, 1976.

[32] Franke, R., "Scattered Data Interpolation: Test of Some Methods," *Mathematics of Computation*, Vol. 38, No. 157, Jan. 1982, pp. 181–199.

[33] Jones, D., "Force Transfer in Aeroelastic Calculations," Univ. of Bristol, Rept. AE047, Bristol, England, U.K., Dec. 2002.

[34] Taylor, N. V., Vio, G. A., Rampurawala, A. M., Allen, C. B., Badcock, K. J., Cooper, J. E., Gaitonde, A. L., Jones, D. P., Woodgate, M. A., and Henshaw, M. J. de C., "Aeroelastic Simulation Through Linear and Nonlinear Analyses: A Summary of Flutter Prediction in the PUMA DARP," *The Aeronautical Journal*,Vol. 110, No. 1107, May 2006, pp. 333–343.

[35] Haase, W., Selmin, V., and Winzell, B. (eds.), *Progress in Computational Flow-Structure Interaction*, Notes on Numerical Fluid Mechanics and Multidisciplinary Design, Vol. 81, Springer–Verlag, Berlin, 2003.

[36] Jones, D. P., and Gaitonde, A. L., "Parallel Multiblock with Moving Meshes for the Calculation of Unsteady Flow Past Complex Configurations," Univ. of Bristol, Rept. AE041, Bristol, England, U.K., Sept. 1999.